Sandwich Double-Decker Lanthanide(III) "Intracavity" Complexes Based on Clamshell-Type Phthalocyanine Ligands: Synthesis, Spectral, Electrochemical, and Spectroelectrochemical Inve...

ARTICLE *in* CHEMISTRY - A EUROPEAN JOURNAL · JUNE 2012

Impact Factor: 5.73 · DOI: 10.1002/chem.201200361 · Source: PubMed

7 AUTHORS, INCLUDING:

V. E. Pushkarev
Russian Academy of Sciences
48 PUBLICATIONS **335** CITATIONS
SEE PROFILE

Nataliya Borisova
Lomonosov Moscow State University
57 PUBLICATIONS **554** CITATIONS
SEE PROFILE

Stanislav A Trashin
University of Antwerp
33 PUBLICATIONS **256** CITATIONS
SEE PROFILE

Nikolai S Zefirov
Tufts Medical Center
1,141 PUBLICATIONS **7,171** CITATIONS
SEE PROFILE

CHEMISTRY
A EUROPEAN JOURNAL

ChemPubSoc
Europe

DOI: 10.1002/chem.201200361

Sandwich Double-Decker Lanthanide(III) "Intracavity" Complexes Based on Clamshell-Type Phthalocyanine Ligands: Synthesis, Spectral, Electrochemical, and Spectroelectrochemical Investigations

Victor E. Pushkarev,*[a, b] Alexander Yu. Tolbin,[a] Fedor E. Zhurkin,[b] Nataliya E. Borisova,[b] Stanislav A. Trashin,[a] Larisa G. Tomilova,*[a, b] and Nikolay S. Zefirov[a, b]

Abstract: Phthalocyanine compounds of novel type based on a bridged bis-ligand, denoted "intracavity" complexes, have been prepared. Complexation of clamshell ligand 1,1′-[benzene-1,2-diylbis(methanediyloxy)]-bis[9(10),16(17),23(24)-tri-*tert*-butylphthalocyanine] ($^{clam,tBu}Pc_2H_4$, **1**) with lanthanide(III) salts $[Ln(acac)_3]\cdot nH_2O$ (Ln = Eu, Dy, Lu; acetylacetonate) led to formation of double-deckers $^{clam,tBu}Pc_2Ln$ (**2a–c**). Formation of high molecular weight oligophthalocyanine complexes was demonstrated as well. The presence of an intramolecular covalent bridge affecting the relative arrangement of macrocycles was shown to result in specific physicochemical properties. A combination of UV/Vis/NIR and NMR spectroscopy, MALDI-TOF mass-spectrometry, cyclic voltammetry, and spectroelectrochemistry provided unambiguous characterization of the freshly prepared bis-phthalocyanines, and also revealed intrinsic peculiarities in the structure–property relationship, which were supported by theoretical calculations. Unexpected NMR activity of the paramagnetic dysprosium complex **2b** in the neutral π-radical form was observed and examined as well.

Keywords: density functional calculations · electrochemistry · lanthanides · phthalocyanines · sandwich complexes

Introduction

Research in the field of rare earth element (REE) sandwich-type phthalocyanine complexes has become increasingly important in recent years due to the development of efficient synthetic approaches[1] that can significantly extend the range of these compounds to previously inaccessible derivatives. The specific electronic structure, characterized by the presence of an intramolecular axial interaction between the ligand π systems, combined with extensive possibilities for functionalization[1,2] allow sandwich complexes to find application in modern high-technology fields.[3] Structural control of their properties is possible by varying the nature of the central metal ion and substituents on the phthalocyanine rings. Thus, the distance between the phthalocyanine decks, as well as their skew angle are determined by the REE ionic radius. In turn, the electronic and steric effects of substituents can influence the orbital and molecular structure of the complexes, and thus affect intrinsic physicochemical properties.

Herein, we report the first synthesis of double-decker phthalocyanines containing an intramolecular spacer group, which covalently binds the macrocycles at the periphery and may contribute to the appearance of structural distortions due to steric effects. Flexible-spacer clamshell-type ligand **1** ($^{clam,tBu}Pc_2H_4$) was chosen as the initial substrate, which became available for research due to the previously developed selective synthesis.[4] Note that ligand **1** exists as an inseparable mixture of regioisomers, which differ in the positions of peripheral substituents. However, this should not significantly affect properties of the resulting compounds, since *tert*-butylated derivatives are known to be among the most versatile substrates in phthalocyanine chemistry. In fact, availability, excellent solubility, and comparatively weak intramolecular interactions in **1** were essential for realization of the synthetic goal of the present study.

To our knowledge, there is a single report on a homoleptic sandwich-type REE phthalocyanine based on a flexible-spacer ligand, namely, a sandwich-clamshell-type heteronuclear lutetium(III) dizinc tetraphthalocyanine,[1d] published to date, although several examples of heteroleptic complexes are known.[5] Thus, formation of REE sandwich

[a] Dr. V. E. Pushkarev, Dr. A. Yu. Tolbin, Dr. S. A. Trashin, Prof. L. G. Tomilova, Prof. N. S. Zefirov
Institute of Physiologically Active Compounds
Russian Academy of Sciences
142432 Chernogolovka, Moscow Region (Russian Federation)
Fax: (+7) 496-524-9508
E-mail: pushkarev@org.chem.msu.ru

[b] Dr. V. E. Pushkarev, F. E. Zhurkin, Dr. N. E. Borisova, Prof. L. G. Tomilova, Prof. N. S. Zefirov
Department of Chemistry
M. V. Lomonosov Moscow State University
119991 Moscow (Russian Federation)
E-mail: tom@org.chem.msu.ru

Supporting information for this article is available on the WWW under http://dx.doi.org/10.1002/chem.201200361.

phthalocyanines based on **1** is of interest both from a synthetic point of view as well as for the studying the impact of the spacer on the physicochemical properties of the resulting compounds.

Results and Discussion

Synthesis of homoleptic lanthanide(III) double-deckers: For the synthesis of double-decker phthalocyanines on the basis of **1**, we used conditions similar to the procedure developed earlier by us for the versatile and highly selective synthesis of symmetrically substituted homoleptic,[6] heteroleptic,[7] and asymmetrical functionally substituted lanthanide sandwich complexes.[1d,f] Thus, complexation of **1** with lanthanide acetylacetonates $[Ln(acac)_3]\cdot n H_2O$ in a melt of cetyl alcohol in the presence of catalytic amounts of lithium methoxide led to formation of the double-deckers **2** (Scheme 1).

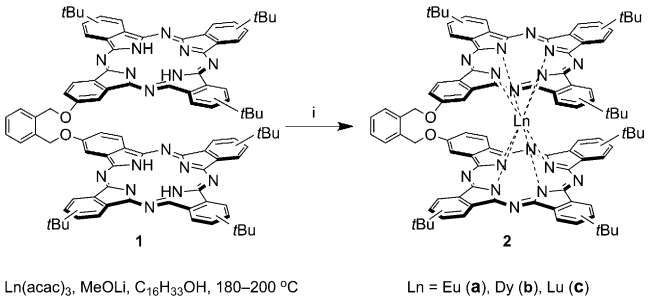

Scheme 1. Synthesis of double-decker complexes.

The role of lithium methoxide in complexation has been discussed previously[1f] with an emphasis on bis-phthalocyanines of the lanthanide middle series. Likewise, in the current study we successfully used this additive to increase the yield of heavy lanthanide complex, namely, lutetium double-decker **2c**, by suppressing byproduct formation. Owing to its bis-ligand nature compound **1** reacts with lanthanide salts in two possible directions. The intramolecular route leads to the target complexes **2**, while the intermolecular one results in formation of an oligophthalocyanine byproduct mixture. To shift the reaction balance towards the former pathway, an excess of solvent was successfully applied along with the addition of base, while the required salt equivalent was introduced into the reaction fractionally. Thus, the proposed scheme led to selective production of double-deckers **2** with good overall yields (Table 1).

Table 1. Yields and high-resolution MALDI-TOF mass spectrometric data for complexes **2**.

	Formula	Yield [%]	$[M]^+$[a]
2a	$C_{96}H_{86}N_{16}O_2Eu$	55	1647.6456 (1647.6332)
2b	$C_{96}H_{86}N_{16}O_2Dy$	61	1658.7860 (1658.6411)
2c	$C_{96}H_{86}N_{16}O_2Lu$	64	1670.7604 (1670.6561)

[a] Calculated values given in parentheses.

Furthermore, complexes of triple-decker nature were detected in trace amounts among the reaction products. On the basis of MALDI-TOF mass spectra and UV/Vis data (Figures S1 and S2 in the Supporting Information) these compounds can be characterized as hexaphthalocyanines **3**

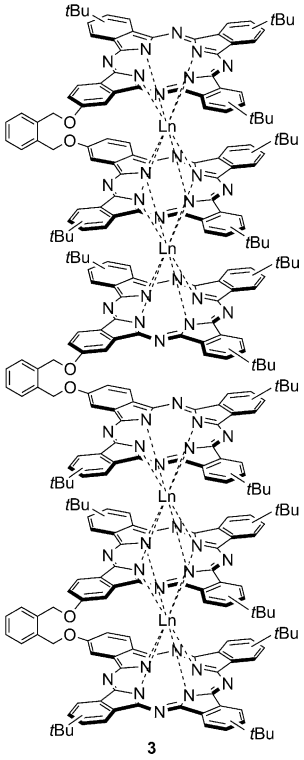

Figure 1. Proposed structure for bis(triple-decker) hexaphthalocyanine co-products **3**.

(Figure 1). In the mass spectra of **3**, low-intensity molecular ion peaks $[M]^+$ are observed, as well as intense clusters of ions generated from $[M]^+$ by fragmentation of an ether bond of the conformationally mobile group linking the triple-decker subunits. Such behavior indicates relatively high lability of this spacer under laser ionization conditions. The UV/Vis spectral line shapes and regularity in their shifts for **3** are in good accordance with corresponding data[1-b,e,6,7,12c] for conventional triple-decker phthalocyanine complexes. The next step in this research will be to shift the reaction selectivity towards the formation of **3**, as well as structural and physicochemical investigations thereof.

The spectral data for the mixture of high molecular weight products formed on interaction of **1** with Eu acetylacetonate are listed in the Supporting Information (Figures S3 and S4). The MALDI-TOF data and UV/Vis absorption spectra indicate the presence of single-, double-, and triple-decker subunits in the oligophthalocyanines, although the detection of molecular ions $[M]^+$ was impeded by their low stability, as observed in the case of hexaphthalocyanine compounds **3**. The possible structure of the lowest molecular weight co-products is presented in Figure S5 of the Support-

ing Information. A high molecular weight product mixture was subjected to gel permeation chromatography to obtain a set of fractions enriched in certain oligophthalocyanines with distribution from high to low molecular weight. The ratio of the UV/Vis absorption bands for these fractions (Figures S6 and S7 in the Supporting Information) correlates well with the structure expected for the corresponding products. Note that their complete identification involving mass spectrometry and NMR spectroscopy requires isolation in an individual state, that is, the specialized study of separation conditions and other associated research, which lies beyond the scope of the present work.

Newly prepared double-decker complexes **2** were characterized by MALDI-TOF mass spectrometry and UV/Vis/NIR electronic absorption and ^{1}H NMR spectroscopy. The MALDI-TOF mass spectra of these compounds (Table 1, Figure 2 and Figures S8–S10 in the Supporting Information) with 2-[(2*E*)-3-(4-*tert*-butylphenyl)-2-methylprop-2-enylidene]malonitrile (DCTB) or 2,5-dihydroxybenzoic acid (DHB) as matrix revealed intense molecular ion peaks with characteristic isotopic patterns that are in good accordance with the simulated spectra (Figure S10 in the Supporting Information). Weak fragmentation of $[M]^+$ due to C–O bond cleavage has a tendency to increase slightly on going from DCTB to DHB matrix. On the other hand, the mass spectrum of ligand **1** shows considerable $[M]^+$ fragmentation,[4] which clearly evidences that intracavity complexation of clamshell-type phthalocyanines with lanthanide ions increases their stability. At the same time, the degree of fragmentation along series **2** tends to increase with increasing REE ionic radius (i.e., interplanar distance), while in the case of conventional double-deckers the inverse relationship has been observed.[8] This reflects enhanced impact of steric effects of the spacer group with increasing interplanar distance.

Electronic absorption spectra: A UV/Vis/NIR spectroscopic study of bis-phthalocyanine complexes **2** in neutral state confirms their intrinsic π-radical nature. The spectra were recorded on CCl_4 solutions of the complexes, and the data are summarized in Table 2. Figure 3 displays the UV/Vis spectra of **2a**,**c**, which are characterized by N-bands at 281–283 nm, split Soret bands in the 324–350 nm region, weaker π-radical blue valence (BV) bands at 462–471 nm, and strong single Q-bands at 666–677 nm that have well resolved vibrational satellites. Furthermore, an expected hypsochromic shift of the absorption bands on going from **2a** (Eu) to **2c** (Lu) is clearly observed. An important feature of the UV/Vis spectra is the increase in full width at half-maximum

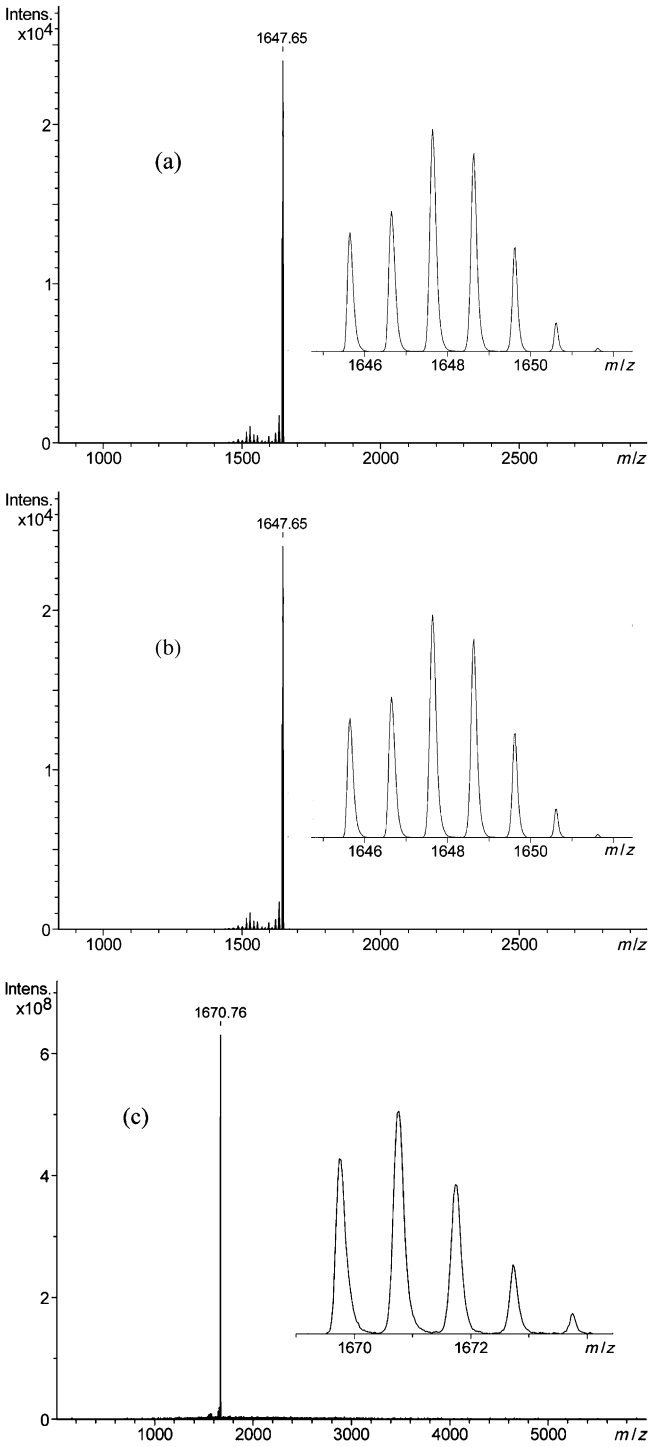

Figure 2. MALDI-TOF mass spectra of compounds **2a**–**c** (a–c, respectively) with DCTB as the matrix; isotopic patterns for the corresponding molecular ions are shown in insets.

Table 2. UV/Vis/NIR electronic absorption data for double-decker complexes **2** in CCl_4.

	λ_{max} [nm] (I/I_{max})[a]							
	N	B (Soret)		π radical	Q_{vib}	Q	RV	IV[b]
2a	281 (0.572)	327 (1.000)	350 (0.690)	471 (0.240)	611 (0.300)	677 (0.946)	910 (0.034)	1431 sh (0.058), 1633 (0.103)
2b	281 (0.607)	324 (1.000)	346 (0.750)	466 (0.258)	606 (0.286)	671 (0.980)	913 (0.046)	1278 sh (0.039), 1426 (0.085), 1565 (0.087)
2c	283 (0.548)	325 (0.945)	344 sh (0.798)	462 (0.243)	602 (0.248)	666 (1.000)	920 (0.053)	1272 sh (0.070), 1398 (0.096), 1524 sh (0.050)

[a] Measured with Helios-α spectrophotometer. [b] Recorded with Hitachi U-4100 instrument.

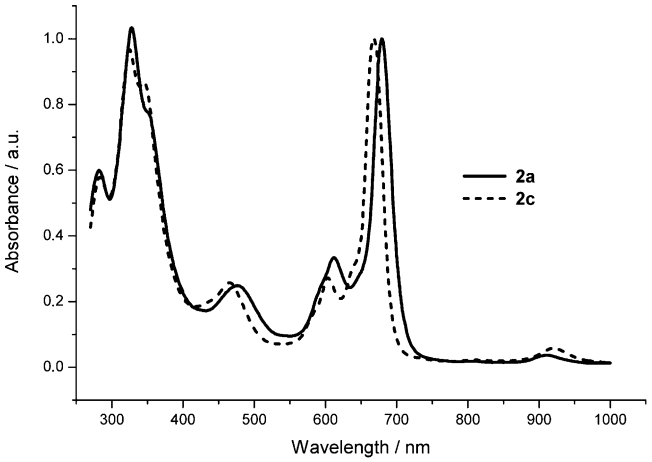

Figure 3. UV/Vis/NIR electronic absorption spectra of compounds **2a** (2.9×10^{-5} M) and **2c** (4.3×10^{-5} M) in CCl_4.

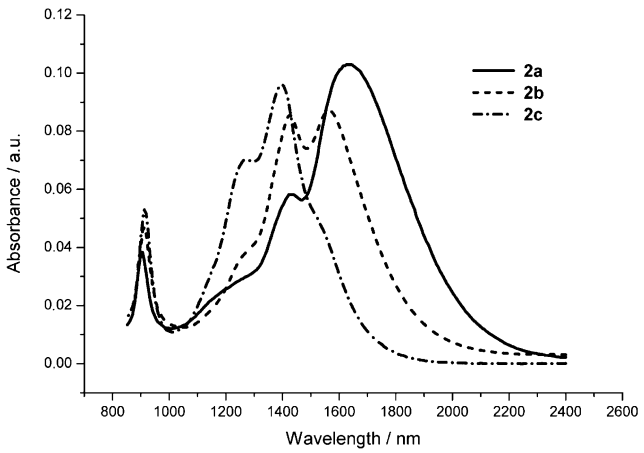

Figure 4. NIR absorption spectra of complexes **2a** (2.9×10^{-5} M), **2b** (3.0×10^{-5} M), and **2c** (4.3×10^{-5} M) in CCl_4.

(FWHM) for the main band maxima on going from **2c** to **2a**, which is most pronounced in the case of the BV band (Table S1 in the Supporting Information). A similar tendency is also observed when comparing the spectra of compounds **2** with the spectra of corresponding bis[2(3),9(10),16(17),23(24)-tetra-*tert*-butylphthalocyanine] lanthanide complexes ($^{tBu}Pc_2Ln$)[9] without intramolecular spacer (Table S1, Figures S11 and S12 in the Supporting Information). We explain the given regularity by taking into account slightly different positions of the individual absorption bands for the isomers of compounds **2** that differ in location of spacer group. Superposition of these bands results in consequent widening of the observed bands. Thus, intrinsic peculiarities of the UV/Vis spectra together with mass spectrometric data indicate increasing in steric effect of the spacer group across the series of compounds **2** with increasing lanthanide ionic radii, which affects the relative arrangement of the macrocycles. Investigation of the NIR absorption spectra (Table 2, Figures 3 and 4) revealed the presence of low-intensity red valence (RV) bands at 910–920 nm and wide intervalence (IV) bands with maxima in the region 1272–1633 nm. A bathochromic shift of the RV band in the series from Eu compound **2a** to Lu complex **2c** is observed, whereas the IV band shifts hypsochromically. Such changes are in good accordance with previously published data for bis-phthalocyanine sandwich complexes[1f,2,3a] and also correspond well to their HOMO–LUMO substructure model.[10]

NMR spectra: Double-decker complexes **2** were prepared as inseparable mixture of isomers for which formation of single crystals suitable for X-ray analysis is impossible. For this reason the role of NMR spectroscopy for structural investigation of **2** is crucial. The ^{1}H NMR spectra of compounds **2** (Figures 5 and 6, Table S2 and Figures S13–S15 in the Supporting Information) were recorded at room temperature in [D$_6$]DMSO in the presence of 1–2 vol% hydrazine hydrate, which reduces the π-radical species to the corresponding monoanionic forms.

The full assignment of NMR signals for compounds **2a**,**c** was made on a basis of published data[1f] for the corresponding double-decker REE complexes with 2-benzyloxy-9,10,16,17,23,24-hexa-*n*-butyl-phthalocyanine ($^{BnO,Bu}PcH_2$) ligand and ^{1}H-^{1}H COSY experiments. Thus, in the spectrum of compound **2a** (Figure 5) the aromatic protons of the phthalocyanine rings H^{Ar} are revealed as a sum of multiplets in the $\delta = 8.5$–12 ppm region, shifted downfield relative to the corresponding signals for ligand **1**[4] due to paramagnetic effect of the Eu^{III} ion. The peaks associated with the α-H^{Ar} protons have intercorrelated signals with the β-H^{Ar} protons (Figure 6) that enabled their assignment. Similarly, on the

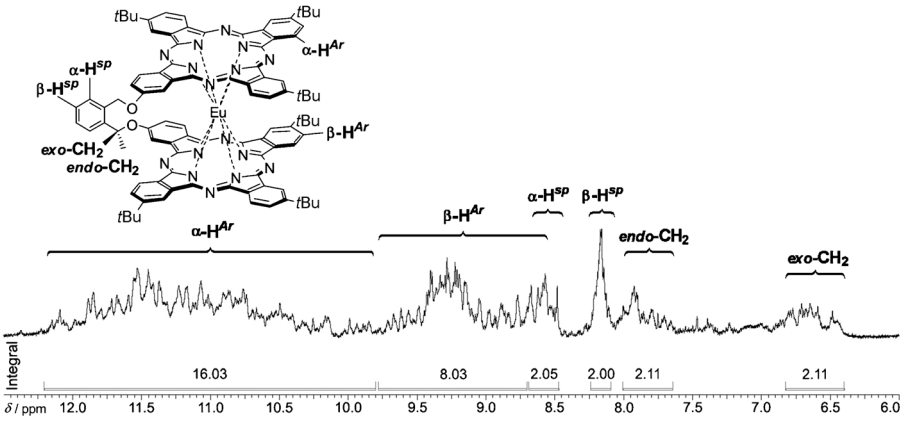

Figure 5. ^{1}H NMR spectrum of compound **2a** (aromatic region) in [D$_6$]DMSO with the addition of 1–2 vol% $N_2H_4{\cdot}H_2O$.

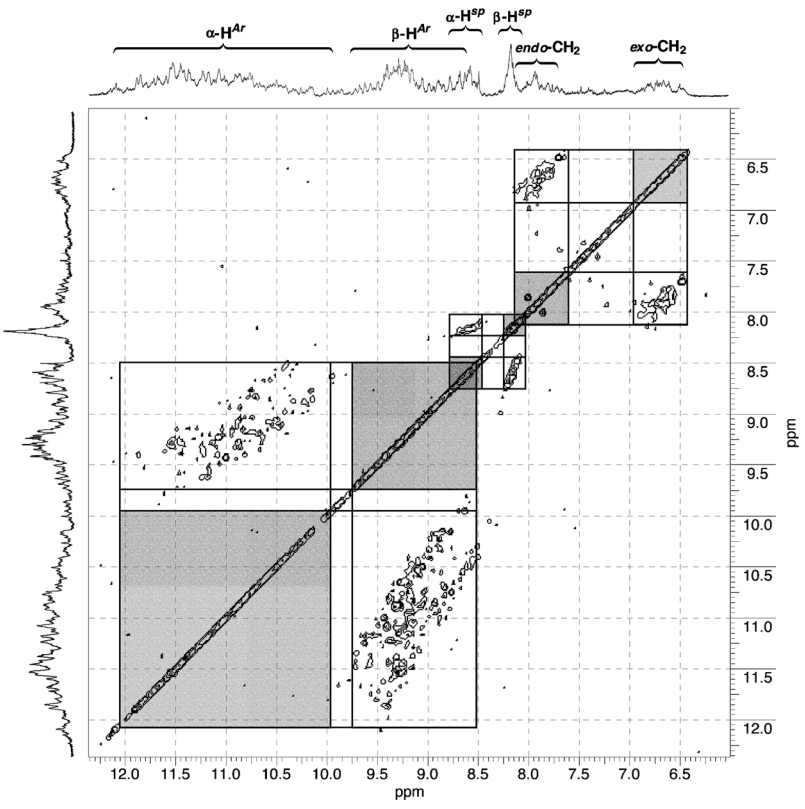

Figure 6. ^{1}H-^{1}H COSY NMR spectrum of compound **2a** (aromatic region) in [D_6]DMSO with the addition of 1–2 vol% $N_2H_4{\cdot}H_2O$.

basis of a 2D NMR spectrum, assignment of the spacer group aromatic (H^{sp}) and aliphatic (CH_2) protons located in regions of 8–9 and 6–8 ppm, respectively, was made. The signals in the aliphatic region at 2–3 ppm belonging to the protons of the *tert*-butyl substituents are also revealed as a sum of singlets. The complex shape of the observed signals, particularly for the CH_2 protons, derives from increased conformational rigidity of molecules **2** compared with the $^{BnO,Bu}Pc_2Ln$ complexes,[1f] which do not bear an intramolecular spacer. A similar approach was applied to fully assign the peaks in the NMR spectrum of lutetium complex **2c** (Figures S13 and S14 in the Supporting Information); note that no additional deshielding of the protons was observed, in contrast to **2a**, due to the diamagnetic nature of the Lu^{III} ion.

The NMR spectrum of dysprosium complex **2c** is of special note. A literature search revealed only a single reference on recording the ^{1}H NMR spectrum of a Dy^{III} double-decker phthalocyanine, obtained by Konami and Hatano,[11] namely, the nonradical unsubstituted tetrabutylammonium salt $[NBu_4]^+[Pc_2Dy]^-$. According to Konami and Hatano, the signals of the phthalocyanine ring protons are observed in the $\delta = 5$–7 ppm region. However, several recent works on triple-decker REE phthalocyanines demonstrated that macrocycle core protons can be revealed in the wide upfield area from $\delta = -10$ up to -80 ppm, which is consistent with strongly paramagnetic nature of the Dy^{III} ion.[12] Bearing this in mind, we tried to record the NMR spectrum of compound **2b** similarly to **2a**,**c** with the complex dissolved in [D_6]DMSO in the presence of reducing agent (Figure S15 in the Supporting Information). In this case, a complex set of poorly resolved signals was observed in the $\delta = -12$ to -23 ppm region as well as a group of signals in the $\delta = -1$ to -7 ppm region, which can be assigned to the protons of *tert*-butyl substituents and CH_2 groups respectively. Phthalocyanine proton signals were not detected for the solution of **2b** under reducing conditions. Surprisingly, the spectrum of a reductant-free solution of **2b** in $CDCl_3$ (Table S2 and Figure S16 in the Supporting Information) showed signals for the H^{Ar} protons, characterized by a strong upfield shift to $\delta = -90$ ppm, and improved resolution of the aliphatic signals. Although we failed to obtain COSY data for the H^{Ar} protons due to considerable broadening of the respective signals, their assignment for **2b** was supported by data obtained under the same conditions for symmetrically substituted Dy^{III} bis(2,3,9,10,16,17,23,24-octa-*n*-butylphthalocyaninate), $^{Bu}Pc_2Dy$, which was synthesized earlier by us (Table S2 and Figures S17 and S18 in the Supporting Information).[13] The ^{1}H NMR spectrum of $^{Bu}Pc_2Dy$ shows a broad singlet at $\delta = -74.21$ ppm assigned to the H^{Ar} protons, while the signals in the $\delta = -8.6$ to -19.6 ppm region are attributed to the aliphatic protons according to the ^{1}H-^{1}H COSY data. Thus, behavior observed for the Dy^{III} bis-phthalocyanine complexes in a reductant-free solution indicates lower paramagnetic contribution to signal broadening for the neutral form compared with the corresponding one-electron reduction product. We explain this effect by magnetic interaction between the 4f electron shell of the Dy^{III} ion and the phthalocyanine π system, which can compensate for the paramagnetism of the π radical. Such an interaction is in accordance with the results obtained by Ishikawa et al.,[14] who demonstrated that dynamic magnetism of 4f single-molecule magnets based on Tb and Dy bis-phthalocyanine compounds can be controlled by a redox reaction on the ligand side without introducing any additional magnetic site or spin system. Although the mechanism of the f–π interaction remains unclear, these observations are noteworthy for research on paramagnetic REE complexes.

Electrochemistry: The redox properties of bis-phthalocyanine complexes **2** were studied in *o*-dichlorobenzene (DCB) by square-wave voltammetry (SWV) with a platinum disk electrode in the potential range from −1.8 to 2.0 V (vs. SCE). The compounds underwent three quasireversible reduction processes, labeled R_1, R_2, and R_3, as well as one reversible and two irreversible oxidation processes, labeled Ox_1, Ox_2, and Ox_3, respectively. Figure 7 shows the SW voltammograms, and Table 3 lists the half-wave potentials ($E_{1/2}$) and differences in potential between the first two oxidation ($\Delta E_{1/2}$) and reduction states ($\Delta E'_{1/2}$).

As shown in Table 3, the redox potentials of both Ox_1 and R_1 are shifted to the cathodic side along the series from **2a** to **2c**, which is in good agreement with previous reports.[15] On the other hand, the potential Ox_2 for Lu complex **2c** is slightly more positive compared to other two compounds. Therefore, the potential difference $\Delta E_{1/2}$ increases with decreasing size of the metal ion, which indicates an increase in π–π interaction. The value of $\Delta E_{1/2}$ reflects the energy separation between the SOMO and the HOMO of the bis-phthalocyanine neutral forms,[15c,e] so it should correlate with the position of the IV band. Our data indeed show such a correlation for both neutral and oxidized forms of compounds **2** (Figure 4, Tables 2 and 4). In turn, the values of the potential R_2 were estimated to be similar for all three complexes. This results in a decrease of the potential difference $\Delta E'_{1/2}$ from 1.182 V for Eu complex **2a** to 1.091 V for Lu compound **2c** (Table 3). The value of $\Delta E'_{1/2}$ was earlier shown to reflect the energy of the HOMO–LUMO gap in the bis(phthalocyanine) one-electron reduced forms.[15c,e] Accordingly, a linear correlation between $\Delta E'_{1/2}$ and the position of the bathochromic component of the Q-band (Q_2) should be observed. Table 4 demonstrates this correlation, since the maxima of the Q_2-band for the complexes **2a** and **2c** were found at 690 and 709 nm respectively. Note that the difference in $\Delta E_{1/2}$ for **2b** and **2c** of nearly 0.11 V is twice that between **2a** and **2b**. According to literature data,[15a,c] the corresponding values for the analogous $^{t\mathrm{Bu}}Pc_2Ln$ complexes are close to each other, in the range of 0.06–0.08 V. This provides evidence that the contribution of the spacer to the π–π interactions increases with decreasing REE ionic radius (i.e., from **2a** to **2c**). Thus the bridge between two phthalocyanine macrocycles in **2** causes slight, yet characteristic, changes in the electrochemical behavior compared with conventional sandwich-type complexes.

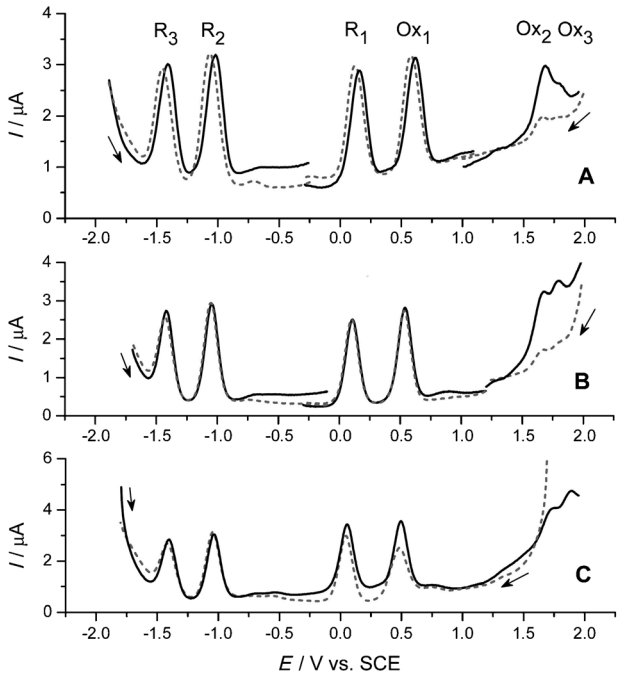

Figure 7. Square-wave voltammograms for reversible couples in DCB containing 0.15 M $[BuN_4][BF_4]$. A) **2a**, B) **2b**, and C) **2c**.

Spectroelectrochemistry: It is well known that sandwich-type phthalocyanine metal complexes reveal strong changes in their electronic absorption spectra from UV up to near-IR region while undergoing oxidation and reduction, and are thus promising electrochromic materials.[3a] UV/Vis spectral changes for complexes **2a** and **2c** during controlled-potential electrolysis at +0.8 and −0.4 V (Figure 8) reflect transformation of the neutral double-decker phthalocyanine

Table 4. Electronic absorption data for the neutral, oxidized, and reduced forms of **2a** and **2c**.

	State	λ_{max} [nm]					
		B (Soret)	π-Radical	Q_{vib}	Q	RV	IV
2a	$[^{clam,t\mathrm{Bu}}Pc_2Eu]^0$	330, 353	482	613	681	912	
	$[^{clam,t\mathrm{Bu}}Pc_2Eu]^+$	323, 365	502	646	724		997
	$[^{clam,t\mathrm{Bu}}Pc_2Eu]^-$	342		535, 593[a]	644, 690 sh		
2c	$[^{clam,t\mathrm{Bu}}Pc_2Lu]^0$	326, 347	470	604	669	919	
	$[^{clam,t\mathrm{Bu}}Pc_2Lu]^+$	320, 359	486	630	704		906
	$[^{clam,t\mathrm{Bu}}Pc_2Lu]^-$	338		513, 580[a]	634, 709		

[a] Approximate position.

Table 3. Half-wave potentials for complexes **2** in DCB.

	$E_{1/2}$ [V] vs. SCE[a]							
	R_3	R_2	R_1	Ox_1	Ox_2	Ox_3	$\Delta E_{1/2}$[b]	$\Delta E'_{1/2}$[c]
2a	−1.431 (−2.077)	−1.043 (−1.689)	0.139 (−0.508)	0.596 (−0.051)	1.663 (1.017)	1.80 (1.15)	1.067	1.182
2b	−1.424 (−2.054)	−1.049 (−1.679)	0.105 (−0.526)	0.537 (−0.094)	1.66 (1.03)	1.79 (1.16)	1.123	1.154
2c	−1.410 (−2.040)	−1.041 (−1.671)	0.050 (−0.581)	0.491 (−0.140)	1.72 (1.09)	1.89 (1.26)	1.229	1.091

[a] Values versus Fc/Fc^+ given in parentheses. [b] $\Delta E_{1/2} = Ox_2 - Ox_1$. [c] $\Delta E'_{1/2} = R_1 - R_2$.

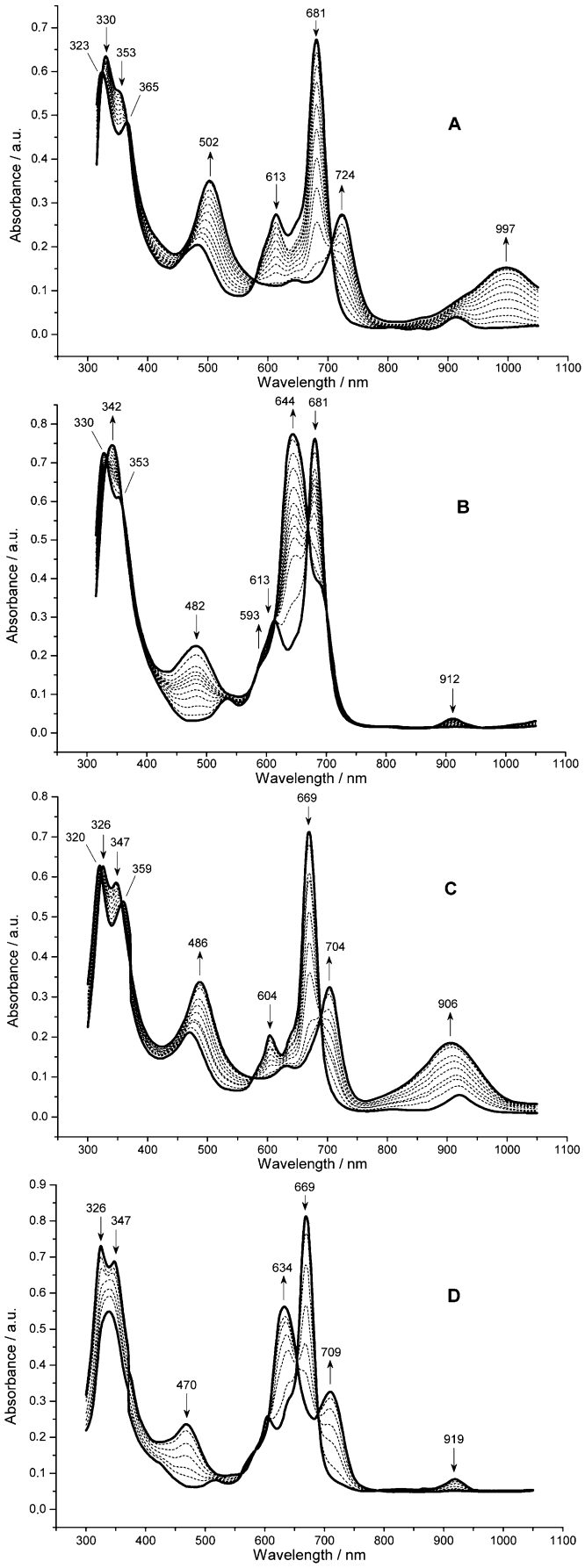

Figure 8. UV/Vis spectral changes for **2a** (1.5×10^{-5} M) and **2c** (2.0×10^{-5} M) in DCB containing 0.2 M $[BuN_4][BF_4]$ during A, C) controlled-potential oxidation (+0.8 V) and B, D) reduction (−0.4 V), respectively.

into the one-electron-oxidized and -reduced forms,[1f,15b,d] respectively. The corresponding band positions are given in Table 4.

Spectral changes in the NIR region are of special note. During oxidation of the neutral form of compound **2c**, a broad band with medium intensity appears near the former position of the RV band. Ishikawa and co-workers[16] earlier observed this band on chemical oxidation of the Pc_2Lu sandwich radical. On the basis of the MCD data and theoretical calculations, Ishikawa et al. assigned this band to the nondegenerate HOMO–LUMO transition, which corresponds to the charge resonance HOMO–SOMO excitation in the neutral form, that is, the IV band. Thus, this is the only band in the UV/Vis/NIR region that shifts to higher energy on oxidation (Figure S19 in the Supporting Information).This band shifts bathochromically by about 90 nm for Eu complex **2a** with respect to the Lu complex **2c**. Such a significant shift is consistent with the behavior of the IV band and thus gives additional support to this assignment. As expected, on reduction of the neutral forms of compounds **2** all of the bands in the NIR region completely disappear. After complete electrolysis, the initial neutral forms of the phthalocyanines were fully recovered by back reduction/oxidation. This reveals good stability of the oxidized and reduced forms in solution. In conclusion, apart from some peculiarities, the electrochemical and spectroelectrochemical behaviors of novel sandwich-clamshell intracavity complexes **2** and classical bis-phthalocyanine compounds are quite similar. This is important, since the data published[17] for spacer-type heteroleptic sandwich complexes, in particular their spectroelectrochemistry, considerably differ from the results reported herein.

Theoretical calculations: Molecular geometry of bis-phthalocyanine complexes is known to be mainly determined by the interplanar distance between the macrocycles, which depends on both the REE ionic radius and total redox state of the compound.[18–20] The nature of peripheral substituents also may affect the geometry to a certain extent,[15e,20] but introduction of an intramolecular spacer group appears to be a more effective pathway for amplification of the steric hindrance. Theoretical calculations (DFT//PBE/TZ2P) were performed for the $^{clam}Pc_2Lu$ compound, which represents the structural analogue of the complex **2c** with *tert*-butyl substituents removed to reduce the calculation time and, more importantly, to clarify the impact of the spacer group (Figure 9). Molecular structures of unsubstituted Pc_2Lu and the "closed" form of the $^{clam}PcH_2$ ligand were also calculated for comparative studies (Figure S20 in the Supporting Information). All optimized structures represent minima on the potential-energy surface (PES), as evidenced by the absence of negative values in their Hessian matrices. Selected param-

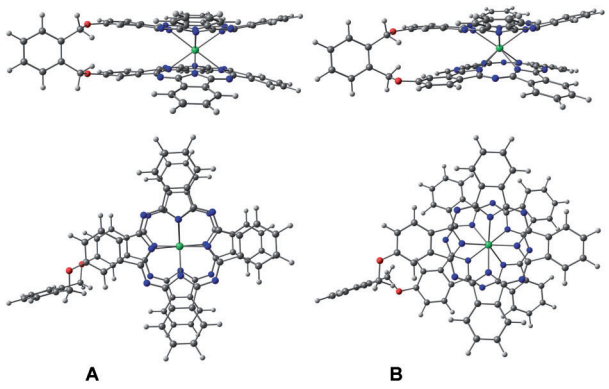

Figure 9. View of the DFT optimized molecular structures of $^{clam}Pc_2Lu$ (simplified model of **2c**). A) Isomer *a*, eclipsed form. B) Isomer *b*, staggered form. Side views are shown at the top, and top views at the bottom.

Table 5. Comparison of calculated d_N,[a] skew angles, and bend angles in Pc_2Lu, "closed" form of $^{clam}PcH_2$ ligand and neutral forms of $^{clam}Pc_2Lu$ isomers *a* and *b*.

	d_N [Å]	Skew angle [°]	Bend angle [°]
$^{clam}Pc_2Lu$ (*a*, eclipsed)	2.946	0.71	3.89
$^{clam}Pc_2Lu$ (*b*, staggered)	2.807	37.01	3.94
$^{clam}Pc_2H_4$	4.064	15.27	0.13
Pc_2Lu[b]	2.769 (2.69)	39.87 (45)	13.57 (13.5)

[a] Distance between the upper and lower planes composed of four N_{iso} atoms. [b] Values given in parentheses correspond to the X-ray data of Ref. [18b].

eters of the optimized geometries are given in Table 5. We define these parameters according to Ref. [18a].

There are two possible isomers of $^{clam}Pc_2Lu$ differing in spacer connection topology: isomer *a*, substituted at positions 2 and 2′, and isomer *b*, linked at positions 2 and 3′ of the phthalocyanine ligands (Figure 9). The DFT optimized structure of isomer *a* is characterized by extremely small skew angle between the ligand planes and therefore termed an eclipsed form (Table 5). Accordingly, isomer *b* is a staggered form, since its skew angle was calculated to be close to that of Pc_2Lu. The ligand moieties of $^{clam}PcH_2$ are also somewhat skewed, while being shifted with respect to each other by 56.13°. The shift angle is defined as the angle between the plane composed of the isoindole nitrogen atoms (N_{iso}) and the line connecting the central points of the two phthalocyanine subunits (Figure S20 in the Supporting Information). Table 5 also shows that interplanar distances of $^{clam}Pc_2Lu$ isomers are very close to that of Pc_2Lu, while the bending angles are smaller due to the presence of the spacer group, which implies certain enhancement of the intramolecular π–π interactions. The staggered form of $^{clam}Pc_2Lu$ is calculated to be more stable than the eclipsed one by about 15 kcal mol^{-1}. This should result in slightly different positions of the main absorption bands in the UV/Vis spectra of these isomers. Therefore, the spectra of their mixture, with superimposed bands, should be characterized by increased FWHM values, as observed in the case of synthesized complexes **2** (Table S1 in the Supporting Information). Moreover, different geometries of the isomers *a* and *b* may be responsible for the increased number of signals in the NMR spectra of compounds **2** besides the influence of the isomers that differ in the positions of *tert*-butyl substituents. Thus, the DFT calculations show a good correlation with the experimental results.

Conclusion

The penetration of lanthanide(III) ions into the inner cavity of a clamshell-type phthalocyanine ligand with formation of double-decker complexes was demonstrated for the first time. Conditions for control of reaction selectivity were found, while high molecular weight oligophthalocyanine coproducts were isolated and characterized as well, and will be the subject of further research. Physicochemical studies on the sandwich bis-phthalocyanine compounds supported by theoretical calculations showed that introduction of an intramolecular spacer group in these compounds can influence their properties by affecting the relative arrangement of macrocycles, and consequently their electronic structure and stability. The paramagnetic dysprosium complex was found to be NMR-active in the neutral π-radical form.

Experimental Section

General: Gel permeation chromatography was accomplished on the polymeric support Bio-Beads S-X1 (BIORAD) with C_6H_6 as eluent. Preparative TLC was performed on flexible plates Merck Silica Gel 60, Merck Silica Gel 60 F_{254}, and Merck Aluminum Oxide F_{254} neutral with C_6H_6 as eluent. The electrolyte $[Bu_4N][BF_4]$ (Sigma-Aldrich) was recrystallized twice from ethyl acetate/hexane (9/1) and dried under vacuum at 80 °C. *o*-Dichlorobenzene (DCB, 99 %, Sigma-Aldrich, HPLC grade) for voltammetric and spectroelectrochemical studies was used as received. All other reagents and solvents were obtained or distilled according to standard procedures. The lanthanide salts $[M(acac)_3]\cdot n H_2O$ were prepared according to literature procedures[21] and dried immediately before use in vacuum desiccator for 5 h at 50 °C. The reactions were monitored by TLC and UV/Vis spectroscopy and were continued until complete disappearance of starting reagents was observed.

Measurements: Electronic absorption (UV/Vis) spectra were recorded with a ThermoSpectronic Helios-α spectrophotometer by using 0.5 cm quartz cells with samples dissolved in CCl_4, C_6H_6,or DCB. UV/Vis/NIR measurements were made with a Hitachi U-4100 instrument by using 0.5 cm quartz cells with the samples dissolved in CCl_4. The concentrations were varied in the range from 1.5×10^{-5} to 4.3×10^{-5} M. MALDI-TOF mass spectra were taken with a VISION-2000 mass spectrometer with 2-[(2*E*)-3-(4-*tert*-butylphenyl)-2-methylprop-2-enylidene]malonitrile (DCTB) or 2,5-dihydroxybenzoic acid (DHB) as matrix. High-resolution MALDI mass spectra were recorded with a Bruker ULTRAFLEX II TOF/TOF instrument with DCTB as the matrix. ^{1}H NMR and ^{1}H-^{1}H COSY spectra were recorded with a Bruker AVANCE 600 spectrometer (600.12 MHz) with samples dissolved in $[D_6]$DMSO to which $N_2H_4\cdot H_2O$ (1–2 vol %) was added at 20 °C, unless otherwise specified. Chemical shifts are given in ppm relative to $SiMe_4$.

Electrochemical measurements were carried out with IPC-Pro (Econix, Moscow, Russia) and EmStat (Palm Instrument BV, Utrecht, the Netherlands) electrochemical interfaces. Cyclic voltammetry (CV) and square-wave voltammetry (SWV) were performed in a conventional three-elec-

trode cell with a Pt-disk (2.0 mm in diameter) working and Pt-foil counterelectrodes. The calomel reference electrode (SCE, 3.5 mol dm^{-3} KCl) was connected to the solution through a salt bridge and a Luggin capillary, the tip of which was placed close to the working electrode. The junction potentials were corrected by a ferrocenium$^+$/ferrocene (Fc^+/Fc) couple each time after a series of measurements. The sample (0.2 mM) was dissolved in a 0.15 M solution of $[Bu_4N][BF_4]$ in DCB, and the solution was purged with argon for 20 min before measurements were taken. The open-circuit potential of the working electrode when immersed in the phthalocyanine solutions was approximately +0.4 V. The scan rate in CVA measurements was varied from 0.05 to 1.00 V s^{-1}. A frequency of 10 Hz and an amplitude potential of 0.05 V were used for SWV. All measurements were performed at ambient temperature (22±1 °C).

Spectroelectrochemical experiments were performed with a quartz electrochemical cell composed of three separated compartments. The rectangular compartment with a path length of 9.3 mm contained a Pt-net working electrode, which was placed near the sidewall of the cell to avoid its interfering with the light beam. A Luggin capillary and a capillary for argon purging were placed close to the working electrode. A reference calomel electrode was connected to the cell through a salt bridge. A Pt counterelectrode with a surface area larger than the area of the working electrode was placed in a separate compartment and connected to the working space through a glass tube fitted with a frit. Sample solutions (1.5×10^{-5} to 2.0×10^{-5} M) contained 0.2 mol dm^{-3} of $[Bu_4N][BF_4]$. Pure argon was passed through the sample solution to remove oxygen and to stir the solution gently during the electrolysis process.

Theoretical calculations: Quantum-chemical calculations were performed with the DFT method. The Perdew–Burke–Ernzerhof (PBE) functional[22] and PRIRODA[23] software package supplied with three exponent TZ2P basis set including twice-polarized Gauss-type functions were used for optimization of the structure geometries. Hessian calculations were used to prove the structures to be minima on the PES. The size of the basis set used was (11s6p2d):[6s3p2d] for C and N, (5s1p):[3s1p] for H, (11s6p2d):[6s3p2d] for O, and (10s10p9d7f):[5s5p3d4f] for Lu.

Preparation of [$^{clam,tBu}Pc_2Ln$] [Ln = Eu (2a), Dy(2b), Lu(2c)]: A mixture of ligand $^{clam,tBu}PcH_2$ (15 mg, 0.01 mmol), MeOLi (2 mg, 0.05 mmol), 0.01 mmol of $[Ln(acac)_3]\cdot n H_2O$, and 150 mg of *n*-hexadecanol (cetyl alcohol) was heated under argon to 180–200 °C for 20–40 min (Scheme 1). The mixture was cooled to room temperature and then diluted with C_6H_6 (5 mL), the insoluble components were filtered off, and the solvents evaporated. The residue was repeatedly washed with boiling MeOH (4× 30 mL) and dried in vacuo. The greenish blue solid that was obtained was dissolved in C_6H_6 and subjected to gel permeation chromatography, from which three different bands were generally collected. The first greenish blue broad band was divided into a set of fractions, each of which by means of UV/Vis and MALDI-TOF data was shown to be enriched with oligophthalocyanines of a certain molecular-weight distribution from heavy to light. The second blue band was shown to contain hexaphthalocyanines **3**, while the last green band contained the target double-decker complexes **2**. Preparative TLC was applied for final purification of the compounds **2** and **3**. Yields of compounds **2** are given in Table 1.

Acknowledgements

We thank Dr. Vladimir M. Senyavin for support in recording the NIR spectra. Financial support from the Programs for fundamental research of the Presidium of the Russian Academy of Sciences ("Development of Synthetic Methods for Chemical Compounds and Creation of New Materials" and "Basis of Fundamental Research in Nanotechnology and Nanomaterials") is gratefully acknowledged. We also thank Joint Supercomputer Center of the Russian Academy of Sciences (www.jscc.ru) for providing the computing resources.

[1] a) V. E. Pushkarev, L. G. Tomilova, Yu. V. Tomilov, *Russ. Chem. Rev.* **2008**, *77*, 875–907; b) A. G. Martynov, O. V. Zubareva, Yu. G. Gorbunova, S. G. Sakharov, A. Yu. Tsivadze, *Inorg. Chim. Acta* **2009**, *362*, 11–18; c) V. E. Pushkarev, A. Yu. Tolbin, A. V. Ryabova, L. G. Tomilova, *Mendeleev Commun.* **2009**, *19*, 24–26; d) A. Yu. Tolbin, V. E. Pushkarev, G. F. Nikitin, L. G. Tomilova, *Tetrahedron Lett.* **2009**, *50*, 4848–4850; e) A. G. Martynov, E. A. Safonova, Yu. G. Gorbunova, A. Yu. Tsivadze, *Russ. J. Inorg. Chem.* **2010**, *55*, 347–354; f) V. E. Pushkarev, A. Yu. Tolbin, N. E. Borisova, S. A. Trashin, L. G. Tomilova, *Eur. J. Inorg. Chem.* **2010**, 5254–5262; g) K. P. Birin, Yu. G. Gorbunova, A. Yu. Tsivadze, *Dalton Trans.* **2011**, *40*, 11539–11549.

[2] a) J. W. Buchler, D. K. P. Ng in *The Porphyrin Handbook, Vol. 3* (Eds: K. M. a.) R. Weiss, J. Fischer in *The Porphyrin Handbook*, Vol. 16 (Eds: K. M. Kadish, K. M. Smith, R. Guilard), Academic Press, San Diego, **2003**, pp. 171–246; b) N. Kobayashi, *Coord. Chem. Rev.* **2002**, *227*, 129–152.

[3] a) J. Jiang, K. Kasuga, D. P. Arnold in *Supramolecular Photosensitive and Electroactive Materials*, Vol. 3 (Ed.: H. S. Nalwa), Academic Press, New York, **2001**, pp. 113–210; b) K.-H. Schweikart, V. L. Malinovskii, A. A. Yasseri, J. Li, A. B. Lysenko, D. F. Bocian, J. S. Lindsey, *Inorg. Chem.* **2003**, *42*, 7431–7446; c) H.-B. Xu, H.-Z. Chen, M.-M. Shi, R. Bai, M. Wang, *Mater. Chem. Phys.* **2005**, *94*, 342–346; d) H. G. Yağlıoğlu, M. Arslan, Ş. Abdurrahmanoğlu, H. Ünver, A. Ermali, Ö. Bekaroğlu, *J. Phys. Chem. Solids* **2008**, *69*, 161–167; e) S. Kyatskaya, J. R. G. Mascaros, L. Bogani, F. Hennrich, M. Kappes, W. Wernsdorfer, M. Ruben, *J. Am. Chem. Soc.* **2009**, *131*, 15143–15151; f) Y. Chen, M. Bouvet, T. Sizun, G. Barochi, J. Rossignol, E. Lesniewska, *Sens. Actuators B* **2011**, *155*, 165–173.

[4] A. Yu. Tolbin, V. E. Pushkarev, L. G. Tomilova, N. S. Zefirov, *Mendeleev Commun.* **2009**, *19*, 78–80.

[5] a) Ş. Abdurrahmanoğlu, A. R. Özkaya, M. Bulut, Ö. Bekaroğlu, *Dalton Trans.* **2004**, 4022–4029; b) Ş. Abdurrahmanoğlu, A. Altindal, A. R. Özkaya, M. Bulut, Ö. Bekaroğlu, *Chem. Commun.* **2004**, 2096–2097; c) T. Ceyhan, M. Korkmaz, M. K. Erbil, Ö. Bekaroğlu, *J. Porphyrins Phthalocyanines* **2005**, *9*, 423–429; d) T. Ceyhan, A. Altindal, A. R. Özkaya, M. K. Erbil, Ö. Bekaroğlu, *Polyhedron* **2007**, *26*, 73–84; e) P. Şen, F. Dumludağ, B. Salih, A. R. Özkaya, Ö. Bekaroğlu, *Synth. Met.* **2011**, *161*, 1245–1254.

[6] V. E. Pushkarev, M. O. Breusova, E. V. Shulishov, Yu. V. Tomilov, *Russ. Chem. Bull.* **2005**, *54*, 2087–2093.

[7] V. E. Pushkarev, E. V. Shulishov, Yu. V. Tomilov, L. G. Tomilova, *Tetrahedron Lett.* **2007**, *48*, 5269–5273.

[8] T. V. Dubinina, R. A. Piskovoi, A. Yu. Tolbin, V. E. Pushkarev, M. Yu. Vagin, L. G. Tomilova, N. S. Zefirov, *Russ. Chem. Bull.* **2008**, *57*, 1912–1919.

[9] L. G. Tomilova, E. V. Chernykh, N. T. Ioffe, E. A. Luk′yanets, *J. Gen. Chem. USSR (Engl. Transl.)* **1983**, *53*, 2594–2601.

[10] C. L. Dunford, B. E. Williamson, E. Krausz, *J. Phys. Chem. A* **2000**, *104*, 3537–3543.

[11] H. Konami, M. Hatano, *Chem. Phys. Lett.* **1999**, *299*, 163–167.

[12] a) D. P. Arnold, J. Jiang, *J. Phys. Chem. A* **2001**, *105*, 7525–7533; b) N. Ishikawa, T. Iino, Y. Kaizu, *J. Phys. Chem. A* **2003**, *107*, 7879–7884; c) A. G. Martynov, O. V. Zubareva, Yu. G. Gorbunova, S. G. Sakharov, S. E. Nefedov, F. M. Dolgushin, A. Yu. Tsivadze, *Eur. J. Inorg. Chem.* **2007**, 4800–4807.

[13] V. E. Pushkarev, A. V. Ivanov, I. V. Zhukov, E. V. Shulishov, Yu. V. Tomilov, *Russ. Chem. Bull.* **2004**, *53*, 554–560.

[14] a) N. Ishikawa, M. Sugita, N. Tanaka, T. Ishikawa, S. Koshihara, Y. Kaizu, *Inorg. Chem.* **2004**, *43*, 5498–5500; b) S. Takamatsu, T. Ishikawa, S. Koshihara, N. Ishikawa, *Inorg. Chem.* **2007**, *46*, 7250–7252; c) N. Ishikawa, Y. Mizuno, S. Takamatsu, T. Ishikawa, S. Koshihara, *Inorg. Chem.* **2008**, *47*, 10217–10219.

[15] a) T. V. Magdesieva, I. V. Zhukov, L. G. Tomilova, E. V. Chernykh, K. P. Butin, *Russ. Chem. Bull.* **1997**, *46*, 2036–2043; b) I. Yilmaz, T. Nakanishi, A. Gurek, K. M. Kadish, *J. Porphyr. Phthalocya.* **2003**, *7*, 227–238; c) P. Zhu, F. Lu, N. Pan, D. P. Arnold, S. Zhang, J. Jiang, *Eur. J. Inorg. Chem.* **2004**, 510–517; d) I. V. Zhukov, V. E. Pushkar-

ev, L. G. Tomilova, N. S. Zefirov, *Russ. Chem. Bull.* **2005**, *54*, 189–194; e) R. Wang, R. Li, Y. Bian, C.-F. Choi, D. K. P. Ng, J. Dou, D. Wang, P. Zhu, C. Ma, R. D. Hartnell, D. P. Arnold, J. Jiang, *Chem. Eur. J.* **2005**, *11*, 7351–7357.

[16] a) N. Ishikawa, Y. Kaizu, *J. Porphyrins Phthalocyanines* **1999**, *3*, 514–521; b) N. Ishikawa, *J. Porphyrins Phthalocyanines* **2001**, *5*, 87–101.

[17] A. Koca, T. Ceyhan, M. K. Erbil, A. R. Özkaya, Ö. Bekaroğlu, *Chem. Phys.* **2007**, *340*, 283–292.

[18] a) N. Koike, H. Uekusa, Y. Ohashi, C. Harnoode, F. Kitamura, T. Ohsaka, K. Tokuda, *Inorg. Chem.* **1996**, *35*, 5798–5804; b) A. De Cian, M. Moussavi, J. Fischer, R. Weiss, *Inorg. Chem.* **1985**, *24*, 3162–3167.

[19] S. Takamatsu, N. Ishikawa, *Polyhedron* **2007**, *26*, 1859–1862.

[20] S. Kahlal, A. Mentec, A. Pondaven, M. L'Her, J.-Y. Saillard, *New J. Chem.* **2009**, *33*, 574–582.

[21] J. G. Stites, C. N. McCarty, L. L. Quill, *J. Am. Chem. Soc.* **1948**, *70*, 3142–3143.

[22] M. Ernzerhof, G. E. Scuseria, *J. Chem. Phys.* **1999**, *110*, 5029–5036.

[23] D. N. Laikov, Yu. A. Ustynyuk, *Russ. Chem. Bull.* **2005**, *54*, 820–826.

Received: February 2, 2012
Revised: April 3, 2012

Please note: Minor changes have been made to this manuscript since its publication in *Chemistry—A European Journal* Early View. The Editor.

Published online: June 19, 2012

